Under similar experimental conditions (1400 °C, 5 h), the pyrolysis of the poly[(dimethylsilylene)diacetylene] metal oxide composites in an argon atmosphere gave high yields of crystalline solid phases that contained the respective metal carbide and SiC. In all cases, the reaction with the metal oxide takes place at lower temperatures than with only carbon. 2) Variation of the poly[(silylene)diacetylene]s allows the modulation of the composition of the final ceramics as summarized for TiO_2 (Table 3). When aryl groups are bonded to the silylene unit, ceramic residues containing higher amounts of TiC result (Table 3, run 3). In contrast, **1c**, a polymer with two dimethylsilylene units, produces a ceramic with a TiC content of 57.1 % (Table 3, run 2).

Table 3. Pyrolysis of poly[(silylene)diacetylene]–TiO_2 composites.

Run	Polymer (equiv)	TiO_2 (equiv)	Ceramic yield [%]	Composition (MC [%])
1	**1a**	(4)	56	3 SiC-4 TiC (72.7)
2	**1c**	(4)	60	6 SiC-4 TiC (57.1)
3	**1e**	(4)	51	SiC-4 TiC (88.9)

Thus, we may expect to prepare a wide range of multiphase ceramics of defined composition. Investigation of the potential of this method and the mechanistic implications are now under progress.

Received: March 17, 1992 [Z 5242 IE]
German version: *Angew. Chem.* **1992**, *104*, 1228

CAS Registry numbers:
SiC, 409-21-2; TiC, 12070-08-5; ZrC, 12070-14-3; B_4C, 12069-32-8; Mo_2C, 12069-89-5; V_4C_3, 12076-63-0; HfC, 12069-85-1; NbC, 12069-94-2.

---

[1] R. Corriu, C. Guérin, B. Henner, A. Jean, T. Kuhlmann, Fr.-A 05567, **1989**; R. Corriu, C. Guérin, B. Henner, A. Jean, F. Garnier, A. Yassar, *Chem. Mater.* **1990**, *2*, 351; *Organometallics*, **1992**, *11*, 2500.

[2] R. Corriu, C. Guérin, B. Henner, A. Jean, H. Mutin, *J. Organomet. Chem.* **1990**, *396*, C35; *Organometallics*, **1992**, *11*, 2507.

[3] A. Jean, *Ph.D. Thesis*, Université Montpellier, **1991**.

[4] S. Ijadi-Magsoodi, T. J. Barton, *Macromolecules* **1990**, *23*, 4485.

[5] SiC metal carbide ceramics have been recently obtained by the pyrolysis of polycarbosilane metal powder composites: D. Seyferth, N. Bryson, D. P. Workman, C. A. Sobon, *J. Am. Ceram. Soc.* **1991**, *74*, 2687.

[6] For the formation of a SiC-TaC ceramic, see: K. Thorne, E. Liimatta, J. D. Mackenzie, *J. Mater. Res.* **1991**, *6* (10), 2199, and references therein.

[7] TiO_2 particle size: < 100 mesh.

[8] K. Su, L. G. Sneddon, *Chem. Mater.* **1991**, *3*, 10.

[9] The pyrolysis experiments were carried out on weighed samples (0.1 to 1 g) of the polymer metal oxide composite which were heated in an aluminum oxide boat (80 × 10 × 10 mm) with a gas-tight aluminium oxide tube (length 100 cm, diameter 30 mm) fitted with glass taps to allow the connection with a vacuum line. The argon flow was maintained at about 50 mL min^{-1}. Experiments were performed in Eurotherm or Carbolite furnaces (heating rate of 10 °C min^{-1} up to 1400 °C; then 5 h at 1400 °C). Ceramic yield = (weight of pyrolysis residue × 100) (weight of pyrolysis carge)$^{-1}$.

[10] SiC and TiC were characterized by X-ray powder diffraction (Phillips diffractometer, $Cu_{K\alpha}$ radiation). The elemental analysis 48.20 % Ti and 21.16 % Si indicates the SiC–TiC phases to be present in a 3:4 ratio.

[11] See, for example: G. Ramis, P. Quintard, M. Cauchetier, G. Busca, V. Lorenzelli, *J. Am. Ceram. Soc.* **1989**, *72*, 1692.

[12] See, for example: R. Jabra, J. Phalippou, M: Prassas, J. Zarzycki, *J. Chim. Phys. Phys. Chim. Biol.* **1981**, *78*, 777; M. Camblor, A. Corma, A. Martinez, J. Pérez-Pariente, *J. Chem. Soc., Chem. Commun.* **1992**, 589, and references therein.

[13] Simultaneous TGA and TDA analyses were performed in a stream of argon (50 mL min^{-1}) with a Netzsch STA thermogravimetric analyzer interfaced with an Anagas 200 Delsi-Nermag mass spectrometer (heating rate 10 °C min^{-1}). TGA and TDA measurements were conducted with the Netzsch SW-STA-311. 001 software on a HP 9000-300 computer.

[14] P. Pascal, *Nouveau Traité de Chimie Minérale*, Masson, Paris; *Gmelin*

(Organoarsonato)polyoxovanadium Clusters: Properties and Structures of the V^V Cluster $[V_{10}O_{24}(O_3AsC_6H_4\text{-}4\text{-}NH_2)_3]^{4-}$ and the V^{IV}/V^V Cluster $[H_2\{V_6O_{10}(O_3AsC_6H_5)_6\}]^{2-}$ **

By *M. Ishaque Khan, Yuanda Chang, Qin Chen, Hakon Hope, Sean Parkin, D. P. Goshorn*, and *Jon Zubieta**

The chemistry of polyoxovanadium clusters incorporating Group 5 elements has witnessed significant growth in recent years. Arsenic–vanadium clusters exhibit a variety of structural types of considerable topological interest[1, 2] and possess a range of stable cluster oxidation states as well as unusual magnetic properties.[3–6] Furthermore, these heteropolyvanadates exhibit a pronounced tendency to form cage structures which may encapsulate neutral molecules or anions, a feature shared with a number of isopolyanions such as $[V_{18}O_{42}(H_2O)]^{12-}$,[7] $[V_{14}O_{42}(SO_4)]^{8-}$,[5] $[H_4V_{18}O_{42}(X)]^{9-}$ (X = Cl, Br, I),[8–10] and $[V_{12}O_{36}(CH_3CN)]^{4-}$[11] and recently described for $[V_{12}As_8O_{40}(HCO_2)]^{n-}$ ($n = 3,5$),[3] $[V_{15}As_6O_{42}(H_2O)]^{6-}$,[4] $[V_{14}As_8O_{42}(SO_4)]^{6-}$,[5] and $[V_{14}As_8O_{42}(0.5\,H_2O)]^{4-}$.[6] A related family of (organophosphonato)polyoxovanadium clusters constitutes a new class of layered compounds which can exhibit useful sorptive and catalytic properties,[12–14] while the molecular polyanions $[H_{12}V_{12}O_{24}(O_3PC_6H_5)_8]^{4-}$[15] and $[H_6V_{16}O_{32}(O_3PCH_3)_8]^{8-}$[16] provide examples of structures displaying cage and "tire" structural motifs, respectively. However, in contrast to this rapid development of the arsenic- and (organophosphonato)polyoxovanadium systems, the chemistry of oxovanadium clusters with organoarsonates $RAsO_3^{2-}$ remains relatively unexplored, although one example of a layered structure $[V_2O_4(C_6H_5AsO_3H)]\cdot H_2O$[17] has been described. In this communication, we report two novel polyoxovanadium structural types found in the "oxidized" cluster **1** and the mixed valence cluster **2**. The structures of these clusters illustrate the dramatic influences of small changes in ligand type upon the overall molecular geometry.

$(TBA)_2(NH_4)_2[V_{10}O_{24}(O_3AsC_6H_4\text{-}4\text{-}NH_2)_3]$ **1**
$(TBA)_2[H_2\{V_6O_{10}(O_3AsC_6H_5)_6\}]\cdot 2\,H_2O$ **2**

$TBA = (n\text{-}C_4H_9)_4N$

Red, parallelepiped crystals of **1** were prepared in approximately 45% yield by heating a mixture of $(NH_4)_2Na_2K_2[V_{10}O_{28}]$, arsanilic acid $4\text{-}NH_2C_6H_4\text{–}AsO(OH)_2$, and (TBA)Br in methanol at reflux for 20 min. X-ray structure analysis of **1**[18] revealed the presence of discrete (TBA) and NH_4^+ ions and a $[V_{10}O_{24}(O_3AsC_6H_4\text{-}4\text{-}NH_2)_3]^{4-}$ ion, whose structure is shown in Figure 1. The overall structure may be described as a $[V_9O_{21}(O_3AsC_6H_4NH_2)_3]^{3-}$ toroid encapsulating a VO_3^- moiety. The toroid consists of three trinuclear $\{V_3O_{13}\}$ units of edge-sharing octahedra with the conventional 60° angle formed by the V centers,[19] which are linked through bridging oxo groups and the arsonato

---

[*] Prof. J. Zubieta, Dr. M. I. Khan, Y. Chang, Dr. Q. Chen
Department of Chemistry, Syracuse University
Syracuse, NY 13244 (USA)

S. Parkin, Prof. H. Hope
Department of Chemistry, University of California, Davis
Davis, CA 95616 (USA)

Dr. D. P. Goshorn
Exxon Research and Development Co.
Annandale, NJ 08801 (USA)

[**] This work was supported by a grant from the National Science Founda-

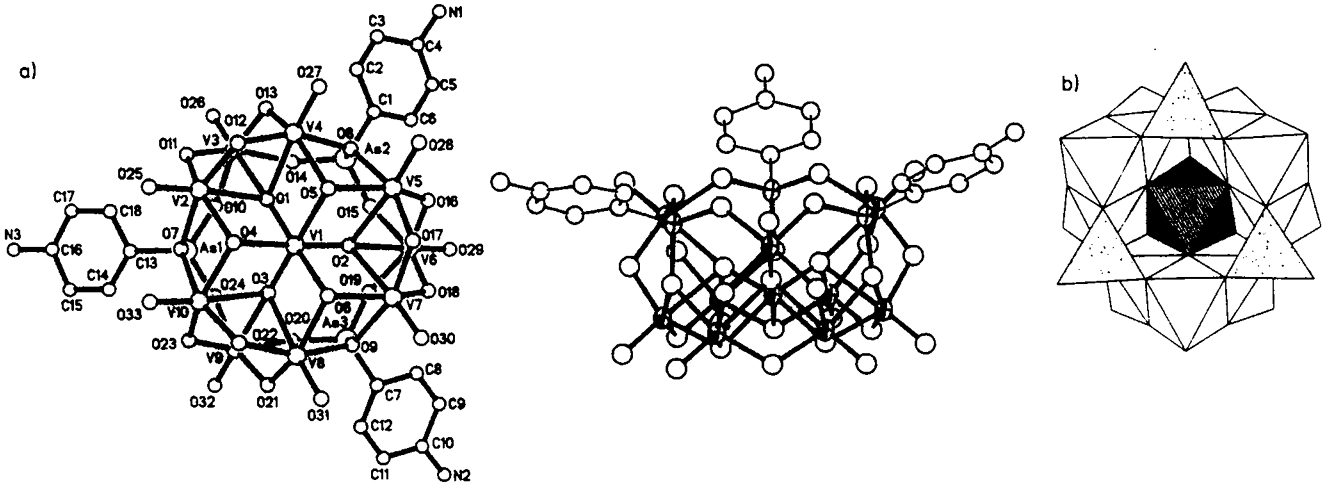

Fig. 1. a) Perspective views of the crystal structure of the anion in **1**. Left: View along the approximate threefold axis of the anion. Right: View perpendicular to this threefold axis. Selected bond lengths [Å] and angles [°]: V(ring)-O(terminal), 1.56(1)–1.61(1); V(ring)-O(μ^2), 1.79(1)–1.86(1); V(ring)-O(μ^3), 1.92(2)–1.99(1); V(ring)-O(μ^4), 2.28(1)-2.33(1); V1-O(μ^3), 2.10(1)–2.20(1); V1-O(μ^4), 1.69(1)–1.71(1); As-O(μ^2), 1.65(2)–1.69(2); As-O(μ^3), 1.72(2)–1.75(2); O1-V1-O6, 166.1(6); O2-V1-O4, 167.1(6); O3-V1-O5, 168.8(6). b) A polyhedral representation of the structure of the anion illustrating the stacking one ring of V octahedra and As tetrahedra, $[V_3(RAsO)_3]^{9+}$, on an Anderson core $[V_7O_{24}]^{13-}$.

ligands. The central vanadium atom V1 is in a highly distorted octahedral environment, in which the metal atom is displaced toward the O1-O2-O3 face; the average V–O(1,2,3) distance is 1.70(2) Å as compared to an average distance of 2.14(2) Å for V–O(4,5,6). This unusual oxometalate arrangement in **1** gives rise to four distinct types of oxo groups: terminal O atoms associated with the V centers of the nine-membered ring, μ^2 oxo groups that bridge V atoms of the $\{V_3O_{13}\}$ units, μ^3 types that link the $\{V_3O_{13}\}$ units to the central vanadium atom, and μ^4 oxo groups which provide both the common vertex for the V octahedra of the trinuclear units and the link to the encapsulated V atom. Each organoarsonate group shares two of its oxygen atoms with vanadium centers of adjacent trinuclear units, while the third is bound to two vanadium centers in neighboring trinuclear units. The anion in **1** exhibits structural features common to polyanions exhibiting a central MO_6 octahedron[20–22] and to ε-Keggin types.[23] The polyhedral representation of Figure 1 b clearly shows the relationship of **1** to the Anderson $\{M_7O_{24}\}$ clusters.[23] The structure of the anion in **1** may be best described as a double layer of polyhedra, one layer composed of the $[V_7O_{24}]^{13-}$ Anderson core and the second consisting of a $[V_3(RAsO_3)_3]^{9+}$ ring which rests on one face of the Anderson core.

Complex **1** undergoes a reversible one-electron reduction at −0.54 V to give the green-brown $[V_{10}O_{24}(O_3AsC_6H_4\text{-}4\text{-}NH_2)_3]^{5-}$ which displays a broad EPR signal centered at $g = 1.95$. In contrast, chemical oxidation of **1** with hydrazines results in multiple-electron transfer coupled to proton transfer to give purple solutions of $[V_{10}O_{21}(OH)_3(O_3AsC_6H_4\text{-}4\text{-}NH_2)_3]^{4-}$. Carefully controlled addition of the hydrazine reagents produces anions of intermediate reduction/protonation states. Such multiple electron–proton transfer processes appear to be characteristic of the chemistry of polyvanadates stabilized by organic ligands.[30]

The reaction of $(NH_4)_2Na_2K_2[V_{10}O_{28}]$ with $C_6H_5AsO(OH)_2$ in the presence of (TBA)Br quite unexpectedly resulted in partial reduction to give **2** as bright green crystals in 65% yield. The structure of **2**[24] consists of discrete (TBA) ions and molecular anions of $[H_2\{V_6O_{10}(O_3AsC_6H_5)_6\}]^{2-}$, shown in Figure 2a. Although the numerous examples of arsonatopolyoxovanadates studied to date in-

that of the anion in **1**, the structure of the anion in **2** consists of a twisted 24-membered ring $\{V_6As_6O_{12}\}$ (Fig. 2b), which is highly distorted by the presence of additional intraring V-O-V and As-O-V bridges; the As-phenyl substituents, the ter-

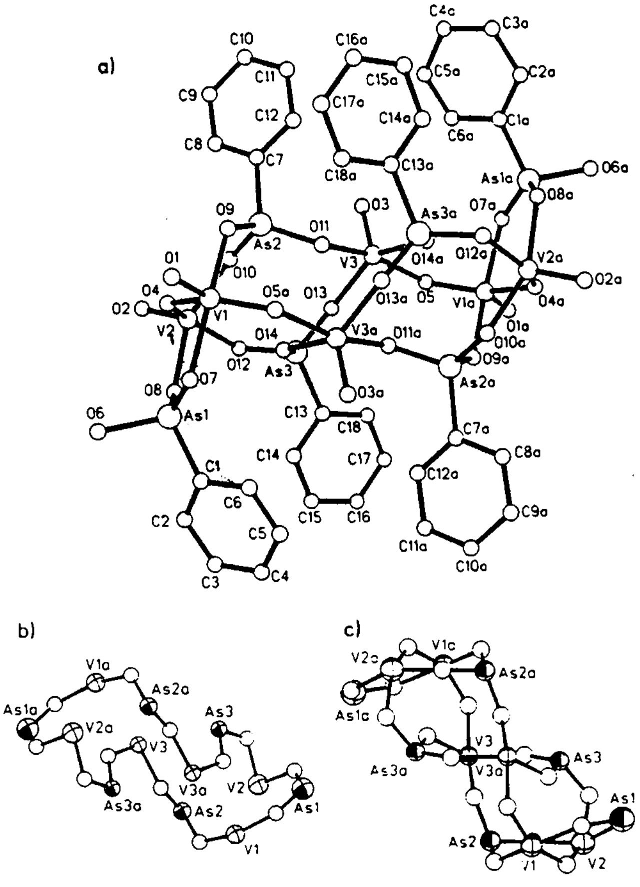

Fig. 2. a) Crystal structure of the anion in **2** (ORTEP). Selected bond lengths [Å]: V1-O1, 1.60(2); V1-O4, 1.97(2); V1-O5, 1.69(2); V1-O7, 2.04(2); V1-O9, 1.94(2); V2-O2, 1.57(3); V2-O4, 1.71(2); V2-O8, 1.98(2); V2-O10, 1.94(2); V2-O12, 1.93(2); V3-O3, 1.59(2); V3-O5, 1.99(2); V3-O11, 2.01(2); V3-O13, 1.99(2); V3-O14, 1.99(2); As1-O6, 1.79(3); all other As-O distances from 1.60(2) to 1.70(2) Å. b) A view of the $\{V_6As_6O_{12}\}$ ring of the anion. c) The

minal oxo groups of the vanadium atoms, and the hydroxyl groups of As1 and As1a project from this central ring. Alternatively, the structure may be described in terms of a layer structure of three $\{V_2As_2O_4\}$ rings connected in a stacking fashion by μ^2 oxo groups, as shown in Figure 2c.

The vanadium centers exhibit square-pyramidal geometry with the standard apical disposition of the terminal oxo groups. Each of the organoarsonate groups is bound to two oxygen atoms and contributes to the formation of the $\{V_2As_2O_4\}$ rings, and four of them employ a third oxygen atom to coordinate to an adjacent ring. The remaining two organoarsonate groups participate in the outermost $\{V_2As_2O_4\}$ rings, while the third oxygen atom of each is a terminal ligand. The latter oxygen atoms, O6 and O6a, are protonated. This assignment is based on the fact that the As3–O6 bond is long relative to the value anticipated for a terminal As=O bond, and the location of one peak in the difference electron density maps is consistent with a hydroxyl proton. The overall anionic charge of 2– requires the presence of four V^V and two V^{IV} centers, an assumption confirmed by potentiometric titration. On the basis of valence sum calculations,[25] the reduced sites are identified as V3 and V3a.

The presence of two reduced centers is confirmed by the magnetic properties of **2**. This compound exhibits behavior characteristic of isolated V_2 units. The temperature dependence of the magnetic susceptibility in the range 4.2 to 300 K follows the Bleany–Bowers equation[26] for isolated dimers containing two $S = 1/2$ cations with isotropic g tensors; the susceptibility displays a maximum at 20 K. The susceptibility data are consistent with extremely weak exchange coupling ($2J = -9.1\ \mathrm{cm^{-1}}$) within vanadium dimers which are effectively isolated from each other. The magnetic data may be compared to that for $(VO^{2+})_2$ systems in which J ranges from -25 to $-250\ \mathrm{cm^{-1}}$.[27] The weak exchange coupling in **2** is similar to that observed for $VO(HPO_4)\cdot 0.5\,H_2O$[28] and $VO(HPO_4)\cdot 2\,H_2O$,[29] salts which possess building blocks made up of two VO^{2+} units with similar exchange networks. Furthermore, in contrast to **1**, **2** undergoes two successive, facile, and reversible one-electron oxidations at +0.09 and +0.46 V, which is consistent with the presence of two readily oxidized V^{IV} centers. Thus, the cluster possesses magnetic and electron-transfer properties suggestive of a dimer $\{V_2O_4(O_3AsC_6H_5)_2\}$ encapsulated and stabilized by sandwiching between two $\{V_2O_5(O_3AsC_6H_5)_2\}$ fragments. While ligand-free polymetalates undergo almost exclusively cathodic processes, the introduction of organic ligands into the polymetalate framework allows the development of a more extensive electrochemistry by stabilizing a variety of "reduced" and mixed valence clusters with modified electron-storage and proton-transfer properties.[30]

The organoarsonate chemistry of vanadium appears to be remarkably diverse, such that relatively minor changes in substituents can produce dramatic structural differences as exemplified by **1** and **2**. Furthermore, their electrochemical and magnetic properties suggest extensive electron storage and coupled electron–proton transfer in the chemistry of clusters of this type.

Experimental Procedure

1: Under an atmosphere of argon, (TBA)Br (2.58 g, 8 mmol) and arsanilic acid (0.868 g, 4 mmol) were placed in a Schlenk tube fitted with a reflux condenser and were then dissolved in methanol (25 mL). $(NH_4)_2Na_2K_2[V_{10}O_{28}]$ (0.56 g, 0.5 mmol) was added, and the resulting suspension was heated at reflux with stirring for 20 min whereupon a clear red-brown solution was obtained. After the hot solution was filtered and cooled to room temperatue, it was stored at 4°C for 20 h. Shiny red crystals of **1** were collected in 45% yield. Satisfactory C,H,N-analysis. IR (KBr): $\tilde{\nu}$ [cm^{-1}] = 3450(s), [illegible], 1624(s), 1597(s), 1500(s), 1479(m), 1457(m), 1307(m), 1181(m), 1092(s), 985(s), 972(vs), 878(s), 790(sh), 733(s), 626(m), 530(m); UV/VIS (CH_3CN): λ_{max} [nm] (ε [$\mathrm{cm^{-1}M^{-1}}$]) = 258 (6.72×10^4), 294 (sh). ^{51}V NMR (CH_3CN, $VOCl_3$ standard): $\delta = -499, -507, -533$; electrochemical parameters (10^{-3} M **1**, 10^{-1} M $(TBA)PF_6$, CH_3CN, ferrocene/ferrocenium standard): −0.54 V (ΔE = 64 mV).

2: A mixture of phenylarsenic acid (0.802 g, 4 mmol), (TBA)Br (2.58 g, 8 mmol), and $(NH_4)_2Na_2K_2[V_{10}O_{28}]$ (0.56 g, 0.5 mmol) in methanol (40 mL) was heated at reflux for 40 min to give a bright green solution. A small amount of insoluble residue was removed by filtration, and the filtrate was evaporated to dryness. The resultant green solid was dissolved in a minimum amount of acetronitrile, carefully layered with 50 mL of pentane, isopropanol, and diethyl ether (1:1:1), and allowed to stand at room temperature for 4 d. Dark green crystals of **2** were isolated in 65% yield. Satisfactory C,H,N-analysis. IR (KBr): $\tilde{\nu}$ [cm^{-1}] = 3058(w), 2962(m), 2874(m), 1482(m), 1440(m), 1382(w), 1094(m), 982(s), 872(vs), 841(vs), 743(s), 691(m), 561(sh), 492(s). UV/VIS (CH_3CN): λ_{max} [nm] (ε [$\mathrm{cm^{-1}M^{-1}}$]) = 240 (2.25×10^4), 275 (sh), 368 (3.30×10^3), 660 (352); magnetic properties: Bleany–Bowers fit: $\chi_0 = -3.74\times10^{-4}\ \mathrm{cm^3mol^{-1}}$, $C_i = 0.0139\ \mathrm{cm^3K\,mol^{-1}}$, $C_d = 0.3036\ \mathrm{cm^3K\,mol^{-1}}$, $2J = -9.1\ \mathrm{cm^{-1}}$; μ_{eff} = 1.73 μ_B; electrochemical parameters (10^{-3} M **2**), 10^{-1} M $(TBA)PF_6$, CH_3CN, ferrocene/ferrocenium standard): +0.09 V (ΔE_p = 62 mV), +0.46 V (ΔE_p = 74 mV).

Received: March 11. 1992 [Z 5235 IE]
German version: *Angew. Chem.* **1992**, *104*, 1236

CAS Registry numbers:
1, 142839-60-9; **2**, 142839-67-6; $4\text{-}NH_2C_6H_4\text{–}AsO(OH)_2$, 98-50-0; $[V_{10}O_{24}(O_3AsO_6H_4\text{-}4\text{-}NH_2)_3]^{5-}$, 142839-61-0; $[V_{10}O_{21}(OH)_3(O_3AsC_6H_4\text{-}4\text{-}NH_2)_3]^{4-}$, 142839-62-1; $(NH_4)Na_2K_2[V_{10}O_{28}]$, 142097-04-9; $C_6H_5AsO(OH)_2$, 98-05-5; $[V_6O_{10}(O_3AsC_6H_5)_6]^{3-}$, 142839-64-3; $[V_6O_{10}(O_3AsC_6H_5)_6]^{3-}$, 142839-63-2.

---

[1] M. T. Pope, A. Müller, *Angew. Chem.* **1991**, *103*, 56; *Angew. Chem. Int. Ed. Engl.* **1991**, *30*, 34.

[2] A. Müller, J. Döring, M. I. Khan, V. Wittneben, *Angew. Chem.* **1991**, *103*, 203; *Angew. Chem. Int. Ed. Engl.* **1991**, *30*, 210.

[3] A. Müller, J. Döring, H. Bögge, *J. Chem. Soc. Chem. Commun.* **1991**, 273.

[4] A. Müller, J. Döring, *Angew. Chem.* **1988**, *100*, 1789; *Angew. Chem. Int. Ed. Engl.* **1988**, *27*, 1721.

[5] A. Müller, J. Döring, *Z. Anorg. Allg. Chem.* **1991**, *595*, 251.

[6] G. Huan, M. A. Greaney, A. J. Jacobson, *J. Chem. Soc. Chem. Commun.* **1991**, 260.

[7] G. K. Johnson, E. O. Schlemper, *J. Am. Chem. Soc.* **1978**, *100*, 3645.

[8] A. Müller, J. Döring, H. Bögge, E. Krickemeyer, *Chimia* **1988**, *42*, 300.

[9] A. Müller, E. Krickemeyer, M. Penk, H.-J. Walberg, H. Bögge, *Angew. Chem.* **1987**, *99*, 1060; *Angew. Chem. Int. Ed. Engl.* **1987**, *26*, 1045.

[10] A. Müller, M. Penk, R. Rohlfing, E. Krickemeyer, J. Döring, *Angew. Chem.* **1990**, *102*, 927; *Angew. Chem. Int. Ed. Engl.* **1990**, *29*, 926.

[11] V. W. Day, W. G. Klemperer, O. M. Yaghi, *J. Am. Chem. Soc.* **1989**, *111*, 5959.

[12] J. W. Johnson, A. J. Jacobson, W. M. Butler, S. E. Rosenthal, J. F. Brody, J. T. Lewandowski, *J. Am. Chem. Soc.* **1989**, *111*, 381.

[13] M. S. Whittingham, A. J. Jacobson, *Intercalation Chemistry*, Academic Press, New York, **1982**.

[14] A. Clearfield, *Inorganic Ion Exchange Materials*, CRC Press, Boca Raton, FL, USA, **1982**.

[15] G. Huan, V. W. Day, A. J. Jacobson, D. P. Goshorn, *J. Am. Chem. Soc.* **1991**, *113*, 3188.

[16] G. Huan, A. J. Jacobson, V. W. Day, *Angew. Chem.* **1991**, *103*, 426; *Angew. Chem. Int. Ed. Engl.* **1991**, *30*, 422.

[17] G. Huan, J. W. Johnson, A. J. Jacobson, J. S. Merola, *Chem. Mater.* **1990**, *2*, 719.

[18] a) **1**: Monoclinic, space group $P2_1/c$ with $a = 13.081(3)$, $b = 23.018(4)$, $c = 27.561(8)$ Å, $\beta = 101.85(1)°$, $V = 8122(3)$ Å^3, $Z = 4$ (ϱ_{calc} = 1.676 g cm^{-1}; $\mu(Cu_{K\alpha}) = 11.41\ \mathrm{mm^{-1}}$), $R = 0.087$ for 5290 reflections with $2\theta < 108.5°$ and $I > 3\sigma(I)$; Siemens P3RA diffractometer with rotating anode, Ni-filtered Cu radiation. The structure was solved using direct methods with the Siemens SHELXTL PLUS package. Further details of the crystal structure investigation may be obtained from the Fachinformationszentrum Karlsruhe, Gesellschaft für wissenschaftlich-technische Information mbH, D-W-7514 Eggenstein-Leopoldshafen 2 (FRG), on quoting the depository number CSD-56316, the names of the authors, and the journal citation.

[19] D. L. Keppert, *The Early Transition Metals*, Academic Press, London, **1972**.

[20] M. T. Pope, *Heteropoly and Isopoly Oxometalates*, Springer, New York, **1983**.

[21] T. J. R. Weakley, *J. Less-Common Met.* **1977**, *54*, 129.

[22] A. Kobayashi, Y. Sasaki, *Chem. Lett.* **1975**, 1123.

[23] M. Ichida, K. Nagai, Y. Sasaki, M. T. Pope, *J. Am. Chem. Soc.* **1989**, *111*, 586.

[24] **2**: Monoclinic, space group $P2_1/c$ with $a = 13.193(2)$, $b = 16.091(4)$, $c = 23.096(5)$ Å, $\beta = 92.96(1)°$, $V = 4896(1)$ Å^3, $Z = 2$ ($\varrho_{calc} = 1.304$ g cm^{-1}; $\mu(\mathrm{Mo}_{K\alpha}) = 10.45$ cm^{-1}), $R = 0.069$ for 2067 reflections with $2\theta < 50°$ and $I > 3\sigma(I)$; Rigaku AFC5S diffractometer, graphite monochromated $\mathrm{Mo}_{K\alpha}$ radiation. The structure was solved using the direct methods routine of the TEXSAN program package [18b].

[25] I. D. Brown, K. K. Wu, *Acta Crystallogr. Sect. B* **1976**, *32*, 1957.

[26] B. Bleany, K. D. Bowers, *Proc. R. Soc. London. A* **1952**, *214*, 451.

[27] A. P. Ginsberg, E. Koubek, H. J. Williams, *Inorg. Chem.* **1966**, *5*, 1656; A. Syamal, *Coord. Chem. Rev.* **1975**, *26*, 309.

[28] J. W. Johnson, D. C. Johnston, A. J. Jacobson, J. F. Brody, *J. Am. Chem. Soc.* **1984**, *106*, 8123.

[29] G. Villeneuve, K. S. Suh, P. Amoros, N. Casan-Pastor, D. Beltran-Porter, *Chem. Mater.* **1992**, *4*, 108.

[30] Q. Chen, D. P. Goshorn, C. P. Scholes, X.-L. Tan, J. Zubieta, *J. Am. Chem. Soc.* **1992**, *114*, in press.

Novel Polyether Copolymers Consisting of Linear and Dendritic Blocks**

By *Ivan Gitsov*, *Karen L. Wooley*, and *Jean M. J. Fréchet**

Polyethylene glycols (PEGs), their derivatives and amphiphilic block copolymers have many applications as phase-transfer reagents,[1] as compounds that could potentially encapsulate other materials,[2] and as emulsifying agents.[3] Their properties arise from the existence of both hydrophilic and hydrophobic parts of the macromolecules. In spite of the promising results achieved up to now, the synthesis of novel polymers and copolymers of that type is still of importance due to the high demand for new materials with defined architecture and improved properties.

Recently, the synthesis of novel dendritic polyethers was reported.[4, 5] Because of their dense, but nonentangled structure these dendrimers are expected to impart unusual properties to other polymeric materials when incorporated in the polymer chain. This report explores the incorporation of these highly branched amorphous and hydrophobic dendrimers in a crystalline hydrophilic PEG as well as the properties of the resulting copolymers.

In a first approach PEG copolymers containing dendritic blocks were prepared by capping the ends of α, ω-bifunctional PEGs with dendrimers possessing a reactive functional group at their core. In order to estimate the influence of the size of the dendritic molecule on the reaction yields and the properties of the copolymers that are formed, dendrimers of the third ([G-3]-Br: **1**) and fourth ([G-4]-Br: **2**) generations were used (Scheme 1).

In order to avoid the association of acidic moieties with PEG[6] and the incomplete conversion[1] of some Williamson-type syntheses, the formation of the PEG dianion in situ by reaction with NaH was carried out in the presence of the dendritic bromide (Scheme 2) as described previously for the synthesis of PEG macromers.[7]

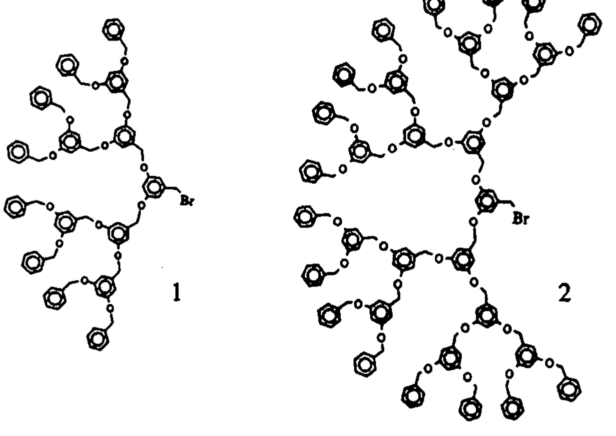

Scheme 1. The dendritic macromolecules employed in the reaction with the polyethylene glycols.

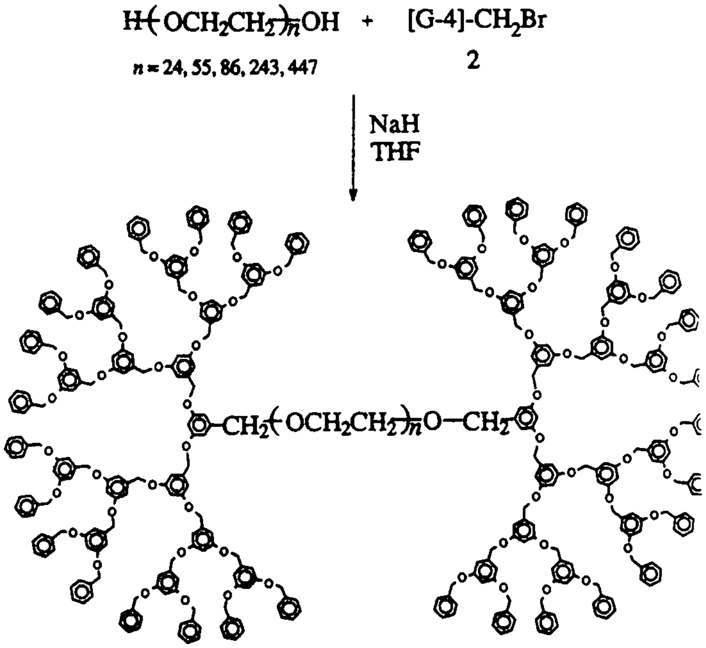

Scheme 2. Synthesis of the copolymers.

In all cases investigated, the end-capping reaction proceeded smoothly at room temperature and was complete within 24 h. The length of the initial PEG block and the size of the dendritic bromide have no influence on the rate of formation of the copolymers. In contrast to the previously reported end-capping reactions of PEGs,[1, 7] the low molar ratio of the dendritic bromides to terminal hydroxyl groups (1.2:1) does not affect the yields, which remain over 90%.

The molecular weights of the starting materials and the resulting block copolymers are listed in Table 1. The molecular weights at the peak apex M_p in the size-exclusion chromatography (SEC) traces are used as characteristic values for each product since they are less affected by low- and high-molecular weight impurities. The molecular weight distribution is calculated as the average of three measurements. It should be noted that most copolymers obtained have narrower molecular weight distributions than the inital PEGs, and all of them have apparent molecular weights lower than the values predicted for triblock copolymers of the type [G-m]-PEG-[G-m] (Table 1, Fig. 1). This difference between calculated and apparent molecular weights increases with the length of the initial PEG block

---

[*] Prof. J. M. J. Fréchet, Dr. I. Gitsov, K. L. Wooley
Baker Laboratory, Department of Chemistry
Cornell University
Ithaca, NY 14853-1301 (USA)

[**] Financial support of this project was provided by National Science Foundation (DMR-8913278) and The William and Mary Greve Foundation (fellowship for I.G.)